Eur. Phys. J. Plus (2023) 138:811
https://doi.org/10.1140/epjp/s13360-023-04428-w

THE EUROPEAN PHYSICAL JOURNAL PLUS

Regular Article

Hp(3) vs TLD-100 for eye lens dosimetry in interventional radiology procedures: a preliminary study

Francesco Manna[1,2,a], **Gianleonardo De Nardellis**[1], **Patrizio Antonio Carmosino**[3], **Fabrizio Ambrosino**[1,4], **Umberto Caruso**[3], **Marco Correra**[3], **Francesco Fiore**[3], **Giuseppe La Verde**[1,4], **Luca Tarotto**[3], **Mariagabriella Pugliese**[1,4]

[1] Department of Physics "E. Pancini", Federico II University, 80126 Naples, Italy
[2] Centro Servizi Metrologici e Tecnologici Avanzati, Federico II University, 80146 Naples, Italy
[3] Interventional Radiology Unit, Istituto Nazionale Tumori, Istituto di Ricovero e Cura a Carattere Scientifico (IRCCS) Fondazione G. Pascale, 80131 Naples, Italy
[4] National Institute of Nuclear Physics, Section of Naples, 80126 Naples, Italy

Received: 19 May 2023 / Accepted: 30 August 2023

Abstract Following the 2013/59/EURATOM Directive, the Italian 101/2020 Decree Law lowered the annual limit on the equivalent dose to eye lens from 150 to 20 mSv for exposed workers, in order to limit the risk of radiation-induced cataract. Such a drastic reduction makes it very important to perform accurate dose monitoring for medical staff that works with ionizing radiation as interventional radiologists and cardiologists. The standard for occupational eye lens dosimetry consists into Hp(3) calibrated dosimeters placed on physicians glasses, next to the eyes. However, this dosimetry system suffers calibration issues, and therefore, the dose is usually extrapolated from extremity or whole body measurements, leading to low accuracy. Chips of thermoluminescent dosimeters TLD-100 and dedicated Hp(3) calibrated dosimeters were placed over a plexiglas (PMMA) phantom to measure the Entrance Surface Air Kerma (K_e) and the eye lens equivalent dose (H) to physician, respectively, during simulated interventional radiology procedures. Values were all below the regulatory limit. Our results show that TLD-100's response seems to be correlated with Hp(3) according to the relationship $K_e = F \times H$, with an average factor $F = 3.9$ mGy/mSv, opening the possibility of using both dosimeters for accurate radiation protection of exposed workers.

1 Introduction

Interventional radiology (IR) is a medical discipline that involves image guidance to perform diagnostic and therapeutic minimally invasive procedures. Interventional techniques have developed extensively over the last decades due to continuous technological progress that has enabled the rise of increasingly sophisticated and advanced medical imaging and fluoroscopy instrumentation and is in rapid evolution [1–5]. The extensive use of imaging results in one of the practices with the highest exposure to ionizing radiation for the physicians [6–9].

This category of workers is chronically exposed to ionizing radiation, which may lead to adverse damage or increased incidence of neoplasia or cancer [10–14]. Following ICRP n.118 [15], there has been increased attention to the occupational exposures of workers involved in these procedures: among the most significant new elements is the lowering of the cumulative dose threshold for cataract induction from 0.5 Gy for fractionated and chronic exposures, to 2 Gy for acute exposures of the eye lens. These indications together the lowering of the equivalent dose limit to the eye lens for exposed workers from 150 to 20 mSv/year were published by Council Directive 2013/59/EURATOM [16]. In Italy, the directive has been transposed into 101/2020 Decree Law [17].

The results of radiobiological and epidemiological studies have shown that in interventional radiology workers the risk of cataracts or brain damage has long been underestimated [18–22].

Cardiologists and interventional radiologists are among the professional workers most exposed to ionizing radiation, with a significant dose contribution to the eye.

The eye and in particular the eye lens is one of the most radiosensitive human tissues [15], and the retina is at risk of suffering serious damage induced by ionizing radiation [23].

Interest in the effects of ionizing radiations on workers is gradually increasing. Although knowledge of eye lens sensitivity has been ongoing for decades, it was only in 2012 that the ICRP n.118 highlighted the real danger of such exposures [15]. However, even though this issue is widely addressed both in regulatory and clinical terms, there is still little compliance on the part of workers in implementing the proper radiation protection precautions and dosimetry protocols. Training about the danger to medical staff

[a] e-mail: francesco.manna@unina.it (corresponding author)

Published online: 15 September 2023

Table 1 Hp(3) calibrated dosimeters specifications provided by Tecnorad s.r.l. with TLD-100 specifications by Harshaw Chemical Company. The acronym ABS stands for Acrylonitrile Butadiene Styrene

Features	Hp(3) calibrated dosimeter	TLD-100 chip
Material and number of detectors	3 LiF:Mg,Cu,P (GR-200A)	1 LiF:Mg,Ti (TLD-100)
Effective atomic number Z_{eff}	8.2	8.2
Filtration	1 mm ABS	None
Measured quantity	Hp(3) = Equivalent dose at a 3 mm depth in tissue (mSv)	R = TLD reading (μC or nC)
Response range in photon energy	13 keV to 3 MeV	>5 keV
Measurement dose range	20 μSv to 500 mSv	10 pGy to 10 Gy
Fading	NA at room temperature	5% per year

related to use of ionizing radiations and the updating of legislative and regulatory statements are required to work in safe conditions [24–26].

A fundamental and, sometimes, underestimated aspect is the technical difficulties related to personal dosimetry at the eye lens. For the evaluation of the equivalent dose to the eye lens, the use of personal dosimeters calibrated in Hp(3) is recommended by ICRP n.103 [19], i.e., which measure a value of absorbed dose at a depth of 3 mm, a value considered appropriate based on the morphology of the eye [27, 28]. A limiting aspect of such dosimeters is the calibration. The usual method for the assessment of Hp(d) is based on the measurement of kerma in air using dosimeters placed on phantom slab and the application of conversion coefficients [29, 30]. Due to these limitations, the dose is typically extrapolated from dosimeters calibrated in Hp(10) or extremity dosimeters using conversion formulae which make the measurements poorly accurate [31, 32].

In this work, thermoluminescent dosimeters (TLDs) were used with Hp(3) calibrated dosimeters to perform measurements in controlled IR procedures [33–36] simulating the worst scenario that is where no radiation protection devices are used during exposures. The methodology involved the use of a Plexiglas phantom to simulate the operator's head [37, 38]. Two different X-ray beam qualities, clinically used for daily procedures, were employed for irradiations. Comparisons between the two dosimeters' results were done with the purpose of finding correlation among the two systems.

2 Materials and methods

Hp(3) dosimeters were used to estimate the eye lens equivalent dose to the first operator in interventional radiology procedures. TLD-100 chips were used as well to estimate the Entrance Surface Air Kerma (K_e) to eyes. Irradiations were performed at the Interventional Radiology Department of Istituto Nazionale Tumori G. Pascale where interventional procedures were simulated on phantoms by using a C-arm under-couch X-ray machine which is used daily.

2.1 Dosimetry system

Hp(3) calibrated dosimeters used for the experiments were LiF:Mg,Cu,P (MCP) provided by Tecnorad s.r.l. Readout was also performed by Tecnorad s.r.l.

TLDs used in the study were Thermo Scientific™ LiF:Mg,Ti chips ($3.2 \times 3.2 \times 0.89$ mm^3) provided by Harshaw Chemical Company.

TLD analysis was performed with Thermo Scientific™ Harshaw TLD™ Model 3500 Manual Reader provided by Harshaw Chemical Company. A pure (99.995%) nitrogen supply was equipped to the reader to suppress chemiluminescence signals not related to irradiations. A 10 s pre-heating to 100 °C followed by a readout to 300 °C with a heating rate of 5 °C/s was used to maximize the TL output [39]. The reading R was obtained by integrating the signal in the region 150–250 °C since the main peak is around 195 °C.

Pre-irradiation annealing was performed with the TLD Annealing Oven "TLD Heat" provided by RadPro with a standard procedure consisted into: 1 h heating at 400 °C, room temperature cooling, 2 h heating at 100°C and room temperature cooling [40, 41].

Characterization of dosimeters was made by evaluating each individual sensitivity factors and calibration factor for energies of interest.

Table 1 illustrates the performance of both Hp(3) calibrated dosimeters and TLDs-100.

2.1.1 Sensitivity characterization

TLDs from a single batch were exposed to a uniform dose distribution of 2 Gy produced by a pair of opposing 6 MV photon beams. Irradiations were performed with Elekta Synergy Linear Accelerator (Elekta Instrument AB Stockholm).

Table 2 Artis Zeego Eco angiography system technical specifications by Siemens Healthcare

Tube voltage	40 kV to 125 kV in 0.1 kV steps
Focal spot size	$0.3 \times 0.3mm^2$ $0.6 \times 0.6mm^2$ $1 \times 1mm^2$
Anode angle	12°
Inherent filtration	2.5 mm Al
Added filtration	0.1, 0.2, 0.3, 0.6, 0.9 mm Cu
Tube current	0.5 mA to 1000 mA in 0.01 mA steps
Pulse time	0.5 ms to 800 ms
Detector type and size	Amorphous silicon flat detector with a 48 cm diagonal entrance plane
Detector resolution	Matrix of 2480 × 1920 pixels with 154 μm pixel size

Each individual sensitivity factor S_i was calculated as the ratio of the reading R_i and the arithmetic mean of all readings of the batch $\overline{R}$:

$$S_i = \frac{R_i}{\overline{R}} \tag{1}$$

2.1.2 Calibration

Dosimeters were calibrated to Cobalt-60 (Co-60) in terms of air kerma, and a correction factor was considered to take into account the over-response of LiF:Mg,Ti to low energy X-rays relatively to Co-60 [42–45].

Calibration to Co-60 was performed at Istituto Superiore di Sanità (ISS) by irradiating TLDs with the Gammacell® 220 provided by Atomic Energy of Canada Limited to dose values of 0.5 Gy, 1.5 Gy and 5 Gy. Moreover, a group of dosimeters from the same batch were used to measure radiation background.

For each exposure, every reading value R_i was corrected using the corresponding sensitivity factor S_i. The arithmetic mean of the readings of background radiation $\overline{R}_{BG}$ was evaluated and subtracted from each measure to obtain the net value for each TLD R_i^{net}:

$$R_i^{\text{net}} = \frac{R_i}{S_i} - \overline{R}_{\text{BG}} \tag{2}$$

For each group of dosimeter exposed to the same dose D, the arithmetic mean R^{net} was calculated.

A graph of net reading vs dose was plotted, and through a linear fit, the calibration factor ($CF_{Co\text{-}60}$) was evaluated as the slope of the line.

TLD response was corrected according to the effective energy E_{eff} of the radiation spectrum to which dosimeters were exposed using correction factors $M(E_{eff})$ calculated by Nunn et al. [43].

2.2 Exposures

Two exposures were performed in a controlled scenario using specific phantoms to simulate both the patient and the head of physician in interventional radiology procedures. During the exposures, we kept the experimental setting unaltered to ensure the replicability.

The angiography room where the irradiations were performed is equipped with the Artis Zeego Eco angiography system by Siemens Healthcare (Erlangen, Germany). System specifications are provided in Table 2.

2.2.1 Phantom

To simulate the operator's head during the irradiation phases and thus, be able to position the dosimeters faithfully under operating conditions, a PMMA phantom of $13 \times 13 \times 9$ cm^3 was used.

To place the phantom and the respective dosimeters correctly and reproducibly, references and positions were marked as showed in Fig. 1a. According to the irradiation procedure, the dosimeters were placed on both right and left sides of the phantom to measure the eye lens dose and the K_e to eyes as showed in Fig. 1b.

2.2.2 Irradiation set-up

Figure 2 shows the set-up used to simulate a real interventional radiology procedure.

Typically, the first operator (i.e., the physician performing the procedure) stands to the right of the supine patient.

The plexiglass phantom was used to simulate the physician's head. The phantom was positioned at 150 cm from the ground. We considered an average physician's height of 170 cm as a reference, bent over the patient during the procedure; this choice was

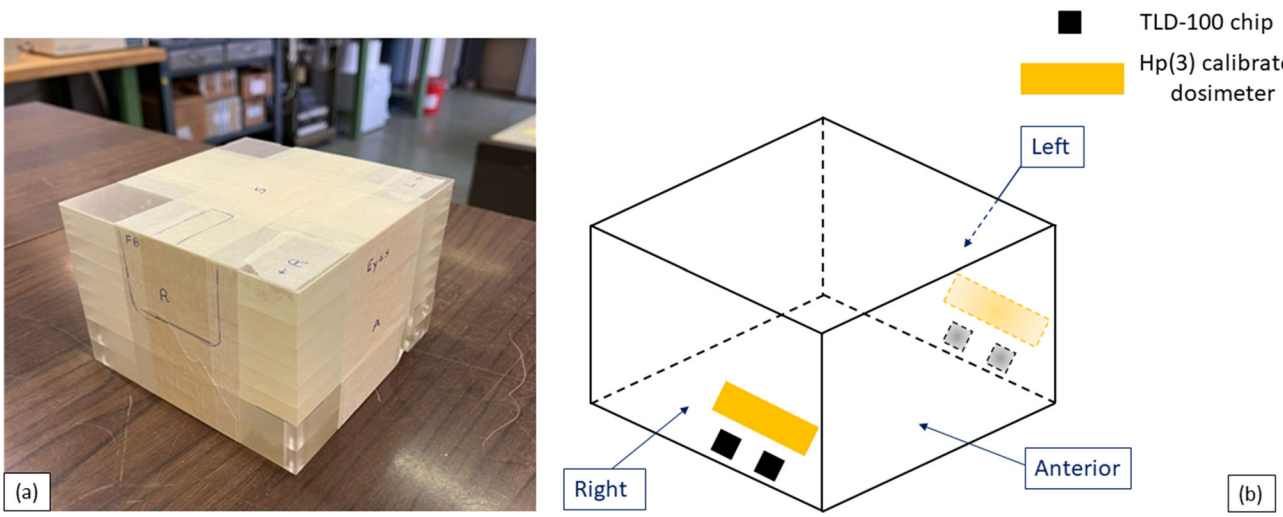

Fig. 1 Phantom detail and dosimeter positioning indication. The left side of the phantom is showed in transparency

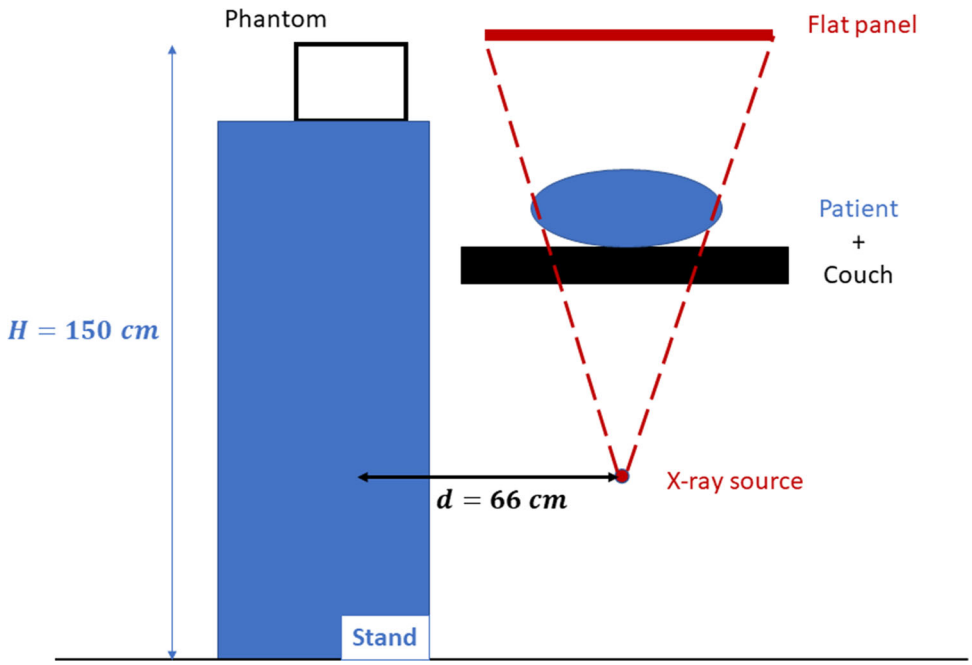

Fig. 2 View from the side of the experimental setup

Table 3 Technical parameters automatically set by Angiography system for both exposures

Exposure	Tube voltage (kV)	Tube current (mA)	Added filtration (mm Cu)	Pulse width (ms)
EXP#1	63	14	0.2	3.3
EXP#2	74	95	0.9	3.9

adopted as it was consistent with the operational requirements [46]. The phantom was placed at 66 cm from the beam axis, simulating a typical distance of the first operator from the beam axis.

At last, to simulate the patient, an anthropomorphic phantom of the pelvis region was used.

In this study, we used a biliary drainage procedure as a reference. We set the source-to-image distance (SID) to 120 cm, the height of the patient table to 90 cm and the field of view (FOV) to 42 cm.

The tube voltage, tube current, filtration, and pulse width [47] were automatically adjusted by the angiographic system according to the patient's anthropometric characteristics using Automatic Exposure Control (AEC) and CARE&CLEARE features; the parameters are shown in Table 3.

Using postero-anterior (PA) X-ray tube angles, which is typical IR condition, two exposures with a 60 min total fluoroscopy time were performed so that the dose was greater of the minimum detectable dose by both types of dosimeters. Keeping the X-ray tube

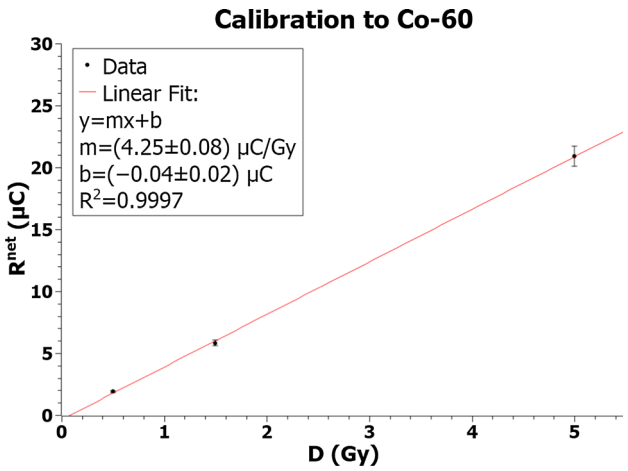

Fig. 3 TLD calibration curve to Co-60 with linear fit. R^2 is the square of Pearson correlation coefficient. Error bars represent the total uncertainty ($k = 2$) from Table 4

Table 4 Measured net readings for each dose point when TLDs were calibrated to Cobalt-60. Relative uncertainties on readings are expressed in Table 4

$D\,(Gy)$	$R^{net}\,(\mu C)$
0.5	1.908
1.5	5.818
5	20.92

Table 5 Uncertainty analysis for TLD calibration to Co-60

Uncertainty source	Type A (%)		Type B (%)
TLD Reproducibility	0.60		
Air-kerma rate determination			1.43
TLD positioning			0.10
PMT linearity correction			1.10
Field uniformity			0.10
Reader stability			0.01
Combined	0.60		1.81
Total ($\boldsymbol{k} = 1$)		1.91	
Expanded ($\boldsymbol{k} = 2$)		3.82	

angles, and operator position unchanged, we modified the patient characteristic adding tissue-equivalent thickness, thus obtaining two different voltage and added filtration values, as reported in Table 3.

3 Results and discussions

Results regarding TLD's characterization will be presented as well as dose measurements from simulated interventional radiology procedures.

3.1 TLD-100 sensitivity and calibration

TLD's sensitivity factors S_i ranged between 0.86 and 1.01, and therefore, no dosimeter was rejected following the methodology proposed by Plato and Miklos [48].

Figure 3 shows the calibration curve obtained for Co-60 with the measured net readings as function of dose provided in Table 4. Uncertainty analysis for calibration is showed in Table 5: TLD reproducibility, air-kerma rate determination, TLD positioning, photomultiplier tube (PMT) linearity correction, field uniformity and reader stability were considered. The TLD reproducibility type A uncertainty was estimated as the percent standard deviation of the mean of all TLD readings used for calibration. Uncertainty in air-kerma rate has been previously estimated by the use of secondary standard dosimetry performed at ISS [49]. The supralinearity index was calculated to take into account the uncertainty contribution for PMT linearity correction [50, 51]. Reader stability uncertainty was considered negligible and assumed to be included in TLD reproducibility [52, 53]. Expanded uncertainty, u, is obtained by multiplying total standard uncertainty with a coverage factor $k = 2$ for a confidence level of 95.5%.

The CF for Co-60 resulted in

Table 6 Cumulative eye lens H and H_{year} estimated with Hp(3) calibrated dosimeters and K_e and $K_{e,\,\mathrm{year}}$ to eyes estimated with TLDs-100 in EXP#1 and EXP#2. Relative expanded uncertainties on TLD-100 measurements are $u = 10\%$

Hp(3) calibrated dosimeter position	EXP#1		EXP#2	
	H(mSv)	H_{year}(mSv)	H(mSv)	H_{year}(mSv)
Left	0.11	8.3	0.22	17
Right	0.09	6.8	0.12	9.0
TLD-100 position	K_{e} (mGy)	$K_{\mathrm{e,year}}$ (mGy)	K_{e} (mGy)	$K_{\mathrm{e,year}}$ (mGy)
Left	0.40	30	0.79	59
Right	0.36	27	0.55	41

$$\mathrm{CF}_{Co-60} = (4.25 \pm 0.16)\frac{\mu C}{Gy}$$

In order to use TLD-100 for dose measurements, an energy correction factor $M(E_{\mathrm{eff}})$ was used to take into account the over-response of LiF:Mg,Ti to lower radiation effective energies. More specifically the absorbed dose $K_{e,i}$ from the i-th dosimeter for IR procedures was calculated as

$$K_{e,i} = \frac{R_i}{S_i \cdot \mathrm{CF}_{\mathrm{Co-60}} \cdot M(E_{\mathrm{eff}})} \tag{3}$$

The effective energy of radiation spectrum used for exposures was computed with TASMICS spreadsheet [54]. For EXP#1, the effective energy resulted in $E_{\mathrm{eff}} = 40\,\mathrm{keV}$, and for EXP#2, it resulted in $E_{\mathrm{eff}} = 54\,\mathrm{keV}$. Therefore, the energy correction factors calculated by Nunn et al. [43] used for the two energies were $M(40\,\mathrm{keV}) = 1.313$ and $M(54\,\mathrm{keV}) = 1.279$. Both factors are calculated with expanded uncertainty $u = 3\%$ ($k = 2$).

3.2 Dose measurements from exposures

For each exposure 2 TLD-100 and 1 Hp(3) dosimeters were used to estimate the dose for each side of phantom, that is for right and left eye lens.

For TLDs-100, the arithmetic mean of the 2 measures was calculated obtaining the average Entrance Surface Air Kerma K_e [55, 56]. Comparisons were made with equivalent dose H measured by Hp(3) calibrated dosimeters.

In order to estimate the equivalent dose per year, the measured values (both from Hp(3) calibrated dosimeters and TLDs-100) were rescaled considering an average time of each IR procedure of 9 min with a total operation number of 500 per year [57]. According to the workload of IR department in our institution, we can therefore estimate the annual equivalent dose per physician, i.e., for a total operation time of 4500 min:

$$H_{\mathrm{year}} = H \cdot \frac{4500}{60} \quad \text{and} \quad K_{e,\mathrm{year}} = K_e \cdot \frac{4500}{60} \tag{4}$$

Results are presented in Table 5.

Uncertainties over TLD-100 measurements were evaluated by considering reproducibility of dosimeters placed on the same side, PMT linearity correction and reader stability for the reading value Ri/Si; uncertainty obtained from calibration to Co-60; and uncertainty on the energy correction factor leading for both exposures to relative expanded uncertainties $u = 10\%$ expressed with one significant figure given the low number of measurements (Table 6).

The measured values reveal a difference in exposure in relation to the position of the operator; according to the experimental evidence attributed to the position of the operator [58], the left eye is more exposed than the right eye for physicians working on the right side of the supine patient [59, 60].

The dose values to the eye lens for the first operator strongly depend on the energies used in clinical practice. The dose value to the lens for the most exposed eye almost doubles by increasing voltage and added filtration.

These values agree with the evidence reported in the literature within estimated uncertainties [61–64].

By analyzing the values recorded by the dosimeters calibrated in Hp(3) against the current limits introduced by the 101/2020 Decree Law [17], it is possible to conclude that in both exposures the first operator is exposed to dose values below the annual limit of 20 mSv, with a value recorded in the left eye, for EXP#2, that is only 3 mSv/year below the regulatory limit.

Comparing to a previous dosimetric study performed in our institute at the same IR department but with a different C-arm X-ray machine [65], it can be noticed how using highly filtered beams with automatic tube potential reduction allows to deliver drastically lower doses to first worker [66, 67].

Table 7 F values for EXP#1 and EXP#2 for both left and right sides. Relative uncertainties are $u = 10\%$

	EXP#1	EXP#2
Phantom side	F(mGy/mSv)	F(mGy/mSv)
Left	3.6	3.5
Right	4.0	4.6

However, despite this improvement, it appears essential to reduce the risk related to radiation exposure, for example by implementing radiation protection training programs and by stimulating the use of devices for radiation protections as leaded glasses or ceiling-suspended screens [68–71].

A comparison of the values recorded by the TLD-100 and Hp(3) calibrated dosimeters shows the possibility of introducing a correlation factor between the cumulative dose to the lens and the entrance surface equivalent dose to eyes.

The correlation was evaluated through the coefficient:

$$F = \frac{K_e}{H} \tag{5}$$

Obtained F values are presented in Table 7.

We measured an average value of 3.8 mGy/mSv, for EXP#1 and an average of 4.1 mGy/mSv for EXP#2.

Different studies have investigated a correlation factor between the dose to the eye lens and dose values recorded by whole body or extremities calibrated dosimeters. Meijer et al. [72] found a correlation factor between the dose to the eye lens and cumulative surface dose on the body dosimeter described by the equation $Hp(3) \simeq 0.25 \cdot Hp(0.07)$, in agreement with results presented in this study where an average factor $\overline{F} = 3.9 \frac{\text{mGy}}{\text{mSv}} \rightarrow 1/\overline{F} = 0.26 \frac{\text{mSv}}{\text{mGy}}$ relates different dosimetry measurements to eye.

A wide variation of correlation factors can be found in the literature; as summarized in the Meijer et al. previously cited study, reported correlation factors were in the range 0.33–1.68 according to methodology (in phantom or in vivo studies), dosimeters arrangement and proprieties [72].

The introduction of a correlation factor allows to evaluate the eye lens dose by estimating its value based on the value recorded by a TLD-100 dosimeter positioned near eyes. This might solve the issue of using Hp(3) dosimeters, which suffer calibration issues, i.e., no regulatory standards for calibration [73].

Exposures should be repeated and replicated using a wider range of energies, which are consistent with those used in clinical practice, in order to find a reliable correlation between dosimeters calibrated in Hp(3) and TLD-100 crystals.

4 Conclusions

This preliminary study investigated the possibility of using a water-equivalent plexiglass phantom to perform radiation protection estimates in IR procedures. Our results show that TLD-100's response in terms of Hp(3) seems to be $K_e(\text{mGy}) = 3.9\left(\frac{\text{mGy}}{\text{mSv}}\right) \times H(\text{mSv})$. This opens the opportunity of performing more studies by using LiF:Mg,Ti crystals which, unlike Hp(3) calibrated dosimeters, are easy to calibrate and to use for exposures to low energy radiation.

In addition, our measured values are in agreement with ones published in the literature proving the effectiveness of phantom measurements.

Even if dose measurements are below the regulatory limits, they emphasize the need of high-quality training about radiation protection and use of collective and individual protection devices in order to guarantee that occupational dose limits are respected and therefore, to assess the safety of exposed workers.

However, more studies will be carried out with the purpose of characterizing TLD-100 response for phantom measurements in IR procedures and the relationship between entrance surface air kerma to eye and lens dose measured by Hp(3) calibrated dosimeters will be studied in detail.

Funding Open access funding provided by Università degli Studi di Napoli Federico II within the CRUI-CARE Agreement.

Data availability statement All data generated or analyzed during this study are included in this published article.

Declarations

Conflict of interest Nothing to declare.

References

1. K. Kandarpa, L. Machan, Handbook of interventional radiologic procedures, eds. (Lippincott Williams & Wilkins, Philadelphia, 2011)
2. T.P. Murphy, G.M. Soares, Semin. Interv. Radiol. (2005). https://doi.org/10.1055/s-2005-869570
3. J. Rösch, F.S. Keller, J.A. Kaufman, J. Vasc, Interv. Radiol. (2003). https://doi.org/10.1097/01.rvi.0000083840.97061.5b
4. M.G. Doherty, Semin. Interv. Radiol. (2019). https://doi.org/10.1055/s-0039-1679951
5. J. Maingard, H.K. Kok, D. Ranatunga, D.M. Brooks, R.V. Chandra, M.J. Lee, H. Asadi, Brit. J. Radiol. (2017). https://doi.org/10.1016/j.ejmp.2020.09.015
6. K.P. Kim, D.L. Miller, S. Balter, R.A. Kleinerman, M.S. Linet, D. Kwon, S.L. Simon, Health Phys. (2008). https://doi.org/10.1097/01.HP.0000290614.76386.35
7. M. Gerić, J. Popić, G. Gajski, V. Garaj-Vrhovac, Mutat. (2019). https://doi.org/10.1016/j.mrgentox.2018.10.001
8. H.L. Kaatsch, J. Schneider, C. Brockmann, M.A. Brockmann, D. Overhoff, B.V. Becker, S. Waldeck, Int J Radiat Biol. (2022). https://doi.org/10.1080/09553002.2021.2020362
9. E. Vano, J.M. Fernandez-Soto, J.I. Ten, R.M. Sanchez Casanueva, (2023) Br. J. Radiol. https://doi.org/10.1259/bjr.20220607
10. G.L. Buchanan, A. Chieffo, J. Mehilli, G.W. Mikhail, F. Mauri, P. Presbitero, L. Grinfeld, A.S. Petronio, K.A. Skelding, A. Hoye, R. Mehran, M.C. Morice, EuroIntervention (2012). https://doi.org/10.4244/EIJV8I6A103
11. L.T. Niklason, M.V. Marx, H.P. Chan, Radiology (1993). https://doi.org/10.1148/radiology.187.3.8497622
12. N.R. Smilowitz, S. Balter, G. Weisz, Cardiovasc. Revasc. Me. (2013). https://doi.org/10.1016/j.carrev.2013.05.002
13. United Nations Scientific Committee on the Effects of Atomic Radiation, Sources And Effects Of Ionizing Radiation. (United Nations, New York, 2010)
14. F. Zakeri, T. Hirobe, K. Akbari Noghabi, Occup. Med. (Lond.) (2010) https://doi.org/10.1093/occmed/kqq062.
15. International Commission on Radiological Protection, ICRP Statement on Tissue Reactions / Early and Late Effects of Radiation in Normal Tissues and Organs – Threshold Doses for Tissue Reactions in a Radiation Protection Context (Elsevier, 2012)
16. The Council Of The European Union, Council Directive 2013/59/EURATOM (Official Journal of the European Union, 2013)
17. Italian Government, Decreto Legislativo 31 luglio 2020, n. 101. (Gazzetta Ufficiale della Repubblica Italiana, 2020)
18. E. Picano, E. Vano, L. Domenici, M. Bottai, I. Thierry-Chef, BMC Cancer (2012). https://doi.org/10.1186/1471-2407-12-157
19. International Commission on Radiological Protection, The 2007 Recommendations of the International Commission on Radiological Protection (Elsevier, 2007)
20. United Nations Scientific Committee on the Effects of Atomic Radiation, Report of the United Nations Scientific Committee on the Effects of Atomic Radiation 2010 (United Nations, New York, 2010)
21. H.K. Moriarty, W. Clements, T. Phan, S. Wang, G.S. Goh, J. Med. Imaging Radiat. Oncol. (2022). https://doi.org/10.1111/1754-9485.13307
22. S. Hattori, H. Monzen, M. Tamura, H. Kosaka, Y. Nakamura, Y. Nishimura, J. Appl. Clin. Med. Phys. (2022). https://doi.org/10.1002/acm2.13532
23. O. Ciraj-Bjelac, M.M. Rehani, K.H. Sim, H.B. Liew, E. Vano, N.J. Kleiman, Catheter Cardiovasc. Interv. (2010). https://doi.org/10.1002/ccd.22670
24. S.G. Barnard, E.A. Ainsbury, R.A. Quinlan, S.D. Bouffler, Br. J. Radiol. (2016). https://doi.org/10.1259/bjr.20151034
25. S. Cornacchia, R. Errico, L. La Tegola, A. Maldera, G. Simeone, V. Fusco, A. Niccoli-Asabella, G. Rubini, G. Guglielmi, Radiol. Med. (2019). https://doi.org/10.1007/s11547-019-01027-7
26. V. D'Avino, L. Angrisani, G. La Verde, M. Pugliese, A. Raulo, G. Sabatino, F. Coppola, Int. J. Environ. Res. Public Health (2019). https://doi.org/10.3390/ijerph16183450
27. M.W. Charles, N. Brown, Phys. Med. Biol. (1975). https://doi.org/10.1088/0031-9155/20/2/002
28. R. Behrens R, J. Radiol. Prot. (2012) https://doi.org/10.1088/0952-4746/32/4/455
29. International Organization for Standardization, X and Gamma Reference Radiations for Calibrating Dosimeters and Doserate Meters and for Determining their Response as a Function of Photon Energy — Part 3: Calibration of Area and Personal Dosimeters and the Measurement of their Response as a Function of Energy and Angle of Incidence. (International Organization for Standardization, Geneva, 1999
30. J.M. Bordy, Radioprotection (2015). https://doi.org/10.1051/radiopro/2015009
31. L. Donadille, E. Carinou, M. Brodecki, J. Domienik, J. Jankowski, C. Koukorava, S. Krim, D. Nikodemova, N. Ruiz-Lopez, M. Sans-Merce, L. Struelens, F. Vanhavere, R. Zaknoune, Radiat. Meas. (2011). https://doi.org/10.1016/j.radmeas.2011.06.034
32. C.J. Martin, Radiat. Prot. Dosimetry. (2009). https://doi.org/10.1093/rpd/ncp168
33. F. Manna, M. Pugliese, F. Buonanno, F. Gherardi, E. Iannacone, G. La Verde, P. Muto, C. Arrichiello, Sensors (2023). https://doi.org/10.3390/s23073592
34. S.M. Ghoneam, K.R. Mahmoud, H.M. Diab, A. El-Sersy, Appl. Radiat. Isot. (2022). https://doi.org/10.1016/j.apradiso.2021.110066
35. C.J. Martin, J.S. Magee, J. Radiol, J. Radio.Prot. (2013). https://doi.org/10.1088/0952-4746/33/2/445
36. G. Mettivier, M. Costa, N. Lanconelli, A. Ianiro, M. Pugliese, M. Quarto, P. Russo, Radiat. Prot. Dosimetry. (2017). https://doi.org/10.1093/rpd/ncw375. (**PMID: 28074018**)
37. G. Gualdrini, F. Mariotti, S. Wach, P. Bilski, M. Denoziere, J. Daures, J.-M. Bordy, P. Ferrari, F. Monteventi, E. Fantuzzi, F. Vanhavere, Radiat. Meas. (2011). https://doi.org/10.1016/j.radmeas.2011.08.025
38. C.J. Martin, Radiat. Prot. Dosimetry. (2016). https://doi.org/10.1093/rpd/ncv431
39. M.F.M. Yusof, N.A. Rashid, R. Abdullah, JSMN **25**(1), 35–44 (2013)
40. C. Furetta, *Handbook of thermoluminescence*, 2nd edn. (World Scientific, Singapore, 2010)
41. V. D'Avino, F. Ambrosino, R. Bedogni, A.I.C. Campoy, G. La Verde, S. Vernetto, C.F. Vigorito, M. Pugliese, Sensors (2022). https://doi.org/10.3390/s22155721
42. S.D. Davis, C.K. Ross, P.N. Mobit, L. Van der Zwan, W.J. Chase, K.R. Shortt, Radiat. Prot. Dosimetry (2003). https://doi.org/10.1093/oxfordjournals.rpd.a006332
43. A.A. Nunn, S.D. Davis, J.A. Micka, L.A. DeWerd, Med. Phys. (2008). https://doi.org/10.1118/1.2898137
44. P. Olko, P. Bilski, J.L. Kim, Radiat. Prot. Dosimetry (2002). https://doi.org/10.1093/oxfordjournals.rpd.a005826
45. A.C. Tedgren, A. Hedman, J.E. Grindborg, G.A. Carlsson, Med. Phys. (2011). https://doi.org/10.1118/1.3633892
46. H. Ishii, K. Chida, K. Satsurai, Y. Haga, Y. Kaga, M. Abe, Y. Inaba, M. Zuguchi, Radiat. Prot. Dosimetry (2019). https://doi.org/10.1093/rpd/ncz027
47. D.L. Smith, J.P. Heldt, G.D. Richards, G. Agarwal, W.G. Brisbane, C.J. Chen, J.D. Chamberlin, D.D. Baldwin, J. Endourol. (2013). https://doi.org/10.1089/end.2012.0213

48. P. Plato, J. Miklos, Health Phys. (1985). https://doi.org/10.1097/00004032-198511000-00019
49. M. Coche, A. Rosati, S. Onori, F. Coninckx, A. Bartolotta, H. Schönbacher, Comparison of high-dose dosimetry systems in accelerator radiation environments (CERN-TIS-RP-205, 1988), https://cds.cern.ch/record/185923/files/CERN-TIS-RP-205.pdf. Accessed 19 May 2023
50. Y.S. Horowitz, Phys. Med. Biol. (1981). https://doi.org/10.1088/0031-9155/26/5/001
51. E.F. Mische, S.W.S. McKeever, Radiat. Prot. Dosimetry (1989). https://doi.org/10.1093/oxfordjournals.rpd.a080548
52. R. Chen, V. Pagonis, eds. (World Scientific, London, 2019)
53. T.H. Kirby, W.F. Hanson, D.A. Johnston, Med. Phys. (1992). https://doi.org/10.1118/1.596797
54. A.M. Hernandez, J.M. Boone, Med. Phys. (2014). https://doi.org/10.1118/1.4866216
55. International Atomic Energy Agency, Dosimetry In Diagnostic Radiology: An International Code Of PractICE (IAEA, 2007)
56. International Commission on Radiological Protection, Radiological Protection in Fluoroscopically Guided Procedures outside the Imaging Department (Elsevier Ltd, 2012)
57. European Society of Radiology, Cardiovascular and Interventional Radiological Society of Europe. Insights Imag. (2019). https://doi.org/10.1186/s13244-019-0698-6
58. International Atomic Energy Agency, Implications for Occupational Radiation Protection of the New Dose Limit for the Lens of the Eye, (IAEA TECDOC SERIES, TECDOC No. 1731, 2013) https://www-pub.iaea.org/mtcd/publications/pdf/te-1731_web.pdf. Accessed 19 May 2023
59. A. Liverani, F. Loffredo, F. Fiore, M. Correra, G. La Verde, M. Pugliese, Nuovo Cimento C (2018) https://doi.org./https://doi.org/10.1393/ncc/i2018-18213-6
60. R.R. Reeves, L. Ang, J. Bahadorani, J. Naghi, A. Dominguez, V. Palakodeti, S. Tsimikas, M.P. Patel, E. Mahmud, J.A.C.C. Cardiovasc, Interv. (2015). https://doi.org/10.1016/j.jcin.2015.03.027
61. M.B. Bellamy, D. Miodownik, B. Quinn, L. Dauer, Radiat. Prot. Dosimetry (2020). https://doi.org/10.1093/rpd/ncaa187
62. E. Carinou, P. Ferrari, C. Koukorava, S. Krim, L. Struelens, Radiat. Prot. Dosimetry (2011). https://doi.org/10.1093/rpd/ncq573
63. Y. Haga, K. Chida, Y. Kaga, M. Sota, T. Meguro, M. Zuguchi, Sci. Rep. (2017). https://doi.org/10.1038/s41598-017-00556-3
64. S. Imai, M. Akahane, Y. Ogata, N. Tanki, H. Sato, K. Tameike, J. Radiol. Prot. (2021). https://doi.org/10.1088/1361-6498/ac091f
65. M. Pugliese, A. Amatiello, M. Correra, V. Stoia, V. Cerciello, V. Roca, F. Loffredo, F. Fiore, G. La Verde, Med. Lav. (2018) https://doi.org/10.23749/mdl.v110i6.7286
66. E. Vañó, L. González, E. Guibelalde, J.M. Fernández, J.I. Ten, Br. J. Radiol. (1998). https://doi.org/10.1259/bjr.71.849.10195011
67. V. Tsapaki, Phys Med. (2020). https://doi.org/10.1016/j.ejmp.2020.09.015
68. U. O'Connor, C. Walsh, A. Gallagher, A. Dowling, M. Guiney, J.M. Ryan, N. McEniff, G. O'Reilly, Br. J. Radiol. (2015). https://doi.org/10.1259/bjr.20140627
69. R.M. Sánchez, E. Vano, J.M. Fernández, F. Rosales, J. Sotil, F. Carrera, M.A. García, M.M. Soler, J. Hernández-Armas, L.C. Martínez, J.F. Verdú, J. Vasc. Interv. Radiol. (2012). https://doi.org/10.1016/j.jvir.2012.05.056
70. R.H. Thornton, L.T. Dauer, J.P. Altamirano, K.J. Alvarado, K. St Germain, S.B. Solomon, J. Vasc. Interv. Radiol. (2010) https://doi.org/10.1016/j.jvir.2010.07.019
71. E. Vaño, L. Gonzalez, J.M. Fernandez, F. Alfonso, C. Macaya, Br. J. Radiol. (2006). https://doi.org/10.1259/bjr/26829723
72. E.J. Meijer, D.W.H. van Zandvoort, M.J.A. Loos, C.M.E.S.N. Tseng, C. van Pul, Phys Med. (2022) https://doi.org/10.1016/j.ejmp.2022.05.012
73. E. Carinou, P. Ferrari, O.C. Bjelac, M. Gingaume, M.S. Merce, U. O'Connor, J. Radiol. Prot. (2015). https://doi.org/10.1088/0952-4746/35/3/R17